Are contributions of emissions to ozone a matter of scale? - A study using MECO(n) (MESSy v2.50)

Mariano Mertens[1], Astrid Kerkweg[2], Volker Grewe[1,3], Patrick Jöckel[1], and Robert Sausen[1]

[1]Deutsches Zentrum für Luft- und Raumfahrt, Institut für Physik der Atmosphäre, Oberpfaffenhofen, Germany
[2] Institut fr Geowissenschaften und Meteorologie, Rheinische Friedrich-Wilhelms-Universität Bonn, Germany
[3] Delft University of Technology, Aerospace Engineering, Section Aircraft Noise and Climate Effects, Delft, the Netherlands

Correspondence: Mariano Mertens (mariano.mertens@dlr.de)

Abstract. Anthropogenic and natural emissions influence the tropospheric ozone budget, thereby affecting air-quality and climate. To study the influence of different emission sources on the ozone budget, often source apportionment studies with a tagged tracer approach are performed. Studies investigating air quality issues usually rely on regional models with a high spatial resolution, while studies focusing on climate related questions often use coarsely resolved global models. It is well known that simulated ozone concentrations depend on the resolution of the model and the resolution of the emission inventory. Whether the contributions simulated by source apportionment approaches also depend on the model resolution, however, is still unclear. Therefore, this study is a first attempt to analyse the impact of the model, the model resolution, and the emission inventory resolution on simulated ozone contributions diagnosed with a tagging method. The differences of the ozone contributions caused by these factors are compared with differences which arise due to different emission inventories. To do so we apply the MECO(n) model system which on-line couples a global chemistry-climate model with a regional chemistry-climate model equipped with a tagging scheme for source apportionment. The results of the global model (300 km resolution) are compared with the results of the regional model at 50 km (Europe) and 12 km (Germany) resolution. Averaged over Europe the simulated contributions of land transport emissions to ground-level ozone differ by 10 % at maximum. For other anthropogenic emission sources the differences are in the same order of magnitude, while the contribution of stratospheric ozone to ground level ozone differs by up to 30 % on average. This suggests that ozone contributions of anthropogenic emission sources averaged on continental scale are rather robust with respect to different models, model and emission inventory resolutions. On regional scale, however, we quantified differences of the contribution of land transport emissions to ozone of up to 20 %. Depending on the region the largest differences are either caused by inter model differences, or differences of the anthropogenic emission inventories. Clearly, the results strongly depend on the compared models and emission inventories and cannot necessarily be generalised, however we show how the inclusion of source apportionment methods can help in analysing inter-model differences.

1   Introduction

Emissions from land transport, industry or shipping contribute largely to global budgets of trace gases like NO_x and O_3, hereby impacting air-quality and climate (e.g., Eyring et al., 2007; Matthes et al., 2007; Hoor et al., 2009; Fiore et al., 2012; Young

et al., 2013; Hendricks et al., 2017; Mertens et al., 2018). To quantify the impacts of these emissions, typically source-receptor relationships are calculated using perturbations or source apportionment methods (e.g., Dunker et al., 2002; Emmons et al., 2012; Stock et al., 2013; Matthias et al., 2016; Huang et al., 2017; Clappier et al., 2017; Butler et al., 2018). Many studies exist quantifying the influence of anthropogenic and natural emission sources (e.g. land transport emissions or lightning) on

5   the ozone budget, but the uncertainties of such analyses are large. Three main sources of uncertainties exist: (1) the emission inventories, (2) model biases/errors, and (3) the resolutions of the models and/or emission inventories. The influences of the first two factors, emission inventories and model biases, have been investigated by multi-scenario and/or multi-model analyses (e.g., Eyring et al., 2007; Hoor et al., 2009; Fiore et al., 2009). Although the influence of the model and emission inventory resolutions onto simulated ozone is well known (e.g. Wild and Prather, 2006; Wild, 2007; Tie et al., 2010; Holmes et al., 2014;

10   Markakis et al., 2015), the impact of the model and emission inventory resolutions on the simulated contributions of specific emission sources to ozone has not yet been systematically investigated in detail. Such an investigation, however, is important as source apportionment studies focusing on climate usually use rather coarsely resolved global climate models (e.g. Wang et al., 1998; Lelieveld and Dentener, 2000; Grewe, 2006; Matthes et al., 2007; Dahlmann et al., 2011; Emmons et al., 2012), while air quality related studies use finer resolved regional models (e.g. Dunker et al., 2002; Li et al., 2012; Kwok et al., 2015;

15   Valverde et al., 2016; Karamchandani et al., 2017). Therefore it is unclear, whether the results on the global and the regional scale are comparable and how large potential errors, caused by the coarse resolution of global models, are. The present study is a first attempt to investigate the influences of the model and of the emission inventory resolutions on the ozone contributions. In detail, we investigate the influences of four different aspects:

- the applied model,

20   - the resolution of the model,

- the resolution of the emission inventory, and

- the emission inventory.

We apply the MECO(n) (**ME**SSy-fied **E**CHAM and **CO**SMO models nested **n** times, e.g. Kerkweg and Jöckel, 2012b; Mertens et al., 2016) model system together with a detailed source apportionment (tagging, Grewe et al., 2017) method. This

25   model system couples on-line the global chemistry-climate model EMAC (**E**CHAM5/**M**ESSy for **A**tmospheric **C**hemistry, Jöckel et al., 2006, 2010) with the regional chemistry-climate model COSMO/MESSy (Kerkweg and Jöckel, 2012a), which consists of the COSMO model (Consortium for Small-scale Modelling) equipped with the MESSy (**M**odular **E**arth **S**ubmodel **Sy**stem, Jöckel et al., 2005, 2010) infrastructure. Due to the MESSy infrastructure, we apply identical submodels for calculating the chemical processes as well as the identical source apportionment method (Grewe et al., 2017) at all nesting steps. Further,

30   the global model provides consistent boundary conditions for the source apportionment to the regional model, allowing a detailed intercomparison of the source apportionment results on different scales. Therefore, we can directly compare the results of the regional and global model, which allows us to estimate uncertainties of the contribution analyses caused by the model,
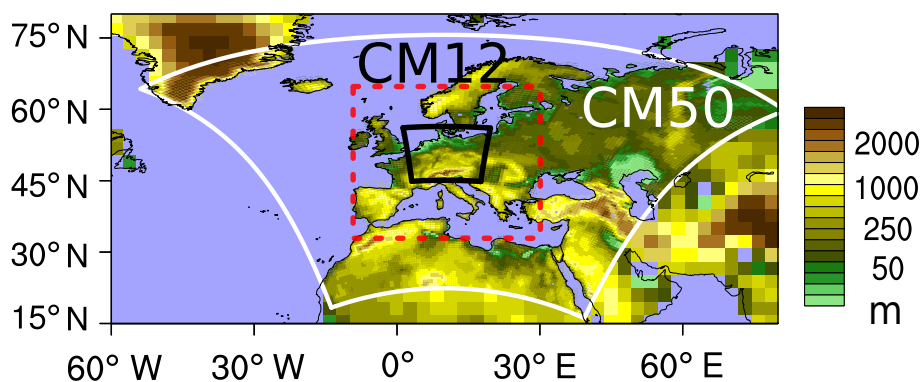
Geoscientific
Model Development
Discussions

Figure 1. Domains of the CM50 (white line) and CM12 (black line) instances. Depicted is the topography of the continents (in m) at the resolution of the corresponding instance. Outside the CM50 domain the topography of EMAC is displayed. Shown is the entire computational domain including the relaxation area. The dashed red square indicates the region analysed in Sect. 4. Figure is largely reproduced from Mertens (2017).

the model resolution and emission inventory resolution. In addition, this model system is, to our knowledge, the first available model system allowing a seamless contribution analysis from global to regional scale.

This paper is organised as follows. First, Sect. 2 gives an overview of the model system followed by an analysis of the ozone production rates simulated by EMAC and COSMO in Sect. 3. In Sect. 4 the differences in the ozone contributions caused by differences of model and emission inventory resolutions are analysed in detail. We provide a quantification of these differences caused by model and emission inventory resolutions in Sect. 5. To set these numbers in to context, we compare these differences with those caused using different emission inventories.

2   Model description and experimental set-up

The MECO(n) model system couples the global chemistry-climate model EMAC on-line with the regional chemistry-climate model COSMO-CLM/MESSy (from now on COSMO/MESSy, Kerkweg and Jöckel, 2012a). COSMO-CLM (COSMO model in Climate Mode) is the community model of the German regional climate research community jointly further developed by the CLM-Community (Rockel et al., 2008). The technical details of MECO(n), as well as meteorological and chemical evaluation are presented in a set of publications (Kerkweg and Jöckel, 2012a, b; Hofmann et al., 2012; Mertens et al., 2016; Kerkweg et al., 2018). Further, the set-up of the simulation applied in the present study is very similar to that described by Mertens et al. (2016), including an evaluation of atmospheric key constituents. Therefore, we present only the most important details of the model system and the set-up. The complete namelist set-up is part of the Supplement.

A MECO(2) set-up with one COSMO/MESSy instance over Europe with a resolution of $0.44° \times 0.44°$ (hereafter named CM50 for COSMO(50km)/MESSy and one instance covering Germany with a resolution of $0.1° \times 0.1°$ (hereafter named CM12 for COSMO(12km)/MESSy was applied (see Fig. 1 for the computational domains). Both COSMO/MESSy instances

use 40 model levels reaching up to a height of 22 km, the damping zone starts at 11 km height. The CM50 instance is driven by EMAC, which is operated at a resolution of T42L31ECMWF, i.e. with a spherical truncation of T42 (corresponding to a quadratic Gaussian grid of approx. $2.8°$ x $2.8°$ in latitude and longitude) with 31 hybrid pressure level in the vertical up to 10 hPa. The boundary conditions for the CM12 instance are provided by the first COSMO/MESSy instance. The applied

5   MESSy version is a modified version of MESSy 2.50, including ECHAM 5.3.02 and COSMO 5.0.0. All changes are included in MESSy 2.51. To facilitate a one to one comparison with observations EMAC is 'nudged' by Newtonian relaxation of temperature, divergence, vorticity and the logarithm of surface pressure (Jöckel et al., 2006) towards ERA-Interim (Dee et al., 2011) reanalysis data of the years 2007 to 2010. Sea surface temperature and sea ice coverage are prescribed as boundary conditions for the simulation set-up from this data source.

10   Due to the MESSy infrastructure the same submodels (e.g. diagnostics or chemical process descriptions) are applied in all model instances (see Table 1 for a list of the most important applied submodels). Most importantly the identical chemical solver (MECCA, Sander et al., 2011) and the identical TAGGING submodel (Grewe et al., 2017) are applied. The simulations are performed using the mechanism 'CCMI-base-01-tag.bat'. This mechanism includes the chemistry of ozone, methane and odd nitrogen. While alkynes and aromatics are not considered, alkenes and alkanes are considered up to C_4. We use the

15   Mainz Isoprene Mechanism (MIM1, Pöschl et al., 2000) for the chemistry of isoprene and some non-methane hydrocarbons (NMHCs). The mechanisms of MECCA and SCAV (scavenging of traces gases by clouds and precipitation, Tost et al., 2006a, 2010) are part of the supplement. The TAGGING submodel allows to calculate the contributions of different emission sources to ozone and the relevant precursors (e.g Mertens et al., 2018). At the lateral and top boundaries of the regional model instances, the tracers of the TAGGING submodel are treated in the same manner as all chemical tracers. Accordingly, the tagged tracers

20   in COSMO/MESSy are relaxed towards the mixing ratios provided by EMAC (or the coarser resolved COSMO instance, respectively) at the lateral and top boundaries. In contrast to this, other tagging schemes, which are used in regional chemistry-climate or chemistry-transport models, usually feature no boundary conditions for the tagged tracers at the lateral (and top) boundaries (e.g. Li et al., 2012; Kwok et al., 2015; Valverde et al., 2016). Therefore, our approach allows for consistent zooming into the area of interest, including an apportionment of the contribution of emissions from different sources to ozone and its

25   relevant precursors across the lateral and top boundaries of the regional model. Especially for chemical species with a long lifetime, such as ozone this is important as large parts of the ozone concentrations at a certain place are influenced by long range transport or subsidence from the stratosphere. If the source apportionment is only performed in the regional model, long range transported ozone can not correctly be attributed to the emission sources themselves.

The Lightning NO_x emissions are calculated in EMAC only using a parametrization based on Price and Rind (1992), which

30   is scaled to a global nitrogen oxide emission rate of ≈ 5 Tg(N) a^{-1} from flashes. The calculated emissions are mapped to COSMO/MESSy and are subsequently emitted there. This approach was chosen as the calculation of lighting-NOx is strongly coupled to the convection parametrisation (e.g. Tost et al., 2007). In different models and/or at different model resolutions convection occurs at different places and/or times and lightning emissions can differ largely. To allow for an easier comparison between the results of different models and at different resolutions we used the same lightning-NO_x emissions. For studies with

35   other scientific questions it would of course be desirable to calculate the lighting-NO_x emissions separately at every resolution.

Emissions of soil-NO_x and biogenic isoprene (C_5H_8) are calculated by the MESSy submodel ONEMIS (Kerkweg et al., 2006b), which uses the parametrisations of Yienger and Levy (1995) for soil-NO_x, and Guenther et al. (1995) for C_5H_8. In contrast to the lightning NO_x emissions, the soil-NO_x and biogenic emissions are calculated in EMAC and COSMO, respectively. This leads to differences in the soil-NO_x and C_5H_8 emissions (see Fig. S5 in the Supplement), influencing the

5 calculation of the contributions. We have chosen this approach, because the land sea masks differ between models and model resolutions. If the emissions calculated by EMAC are simply emitted in the finer resolved COSMO/MESSy model, some of the emissions would occur over sea (or vice versa). This could lead to artificial errors in the contribution analyses. In EMAC, the isoprene emissions calculated by ONEMIS are scaled with a factor of 0.6 (following Jöckel et al., 2006) and in COSMO with 0.45 (following Mertens et al., 2016).

10 For the present study, four different simulations were performed which are named *REF*, *ET42*, *EBIO*, and *EVEU* (see Table 2). The set-up for EMAC is identical in all simulations using the MACCity emission inventory (Granier et al., 2011) with a resolution of $0.5° \times 0.5°$. For the COSMO model instances, however, the emission inventories as well as the resolution of the emission inventories are varied systematically in the different simulations as described below.

In the *REF* simulation, the same MACCity inventory is applied in EMAC and COSMO, using the finest possible resolution

15 in every model instance. This simulation serves as reference, in order to disentangle effects of the resolution of the model from that of the resolution of emission inventories, and the different anthropogenic emission inventories. For the *ET42* simulation, the MACCity emissions are transformed to the coarse grid of EMAC (T42), to investigate the impact of the resolution of the emission inventory. To study the influence of the different on-line calculated emissions of soil-NO_x and isoprene, the simulation *EBIO* is performed. Here, the biogenic emissions calculated by EMAC are mapped down to COSMO and applied

20 instead of the biogenic emissions calculated by COSMO itself. In this case the C_5H_8 emissions in COSMO are also scaled by 0.6. Finally, a different emission inventory for the emission sources shipping, land transport and anthropogenic non-traffic is used in the simulation *EVEU*. This emission inventory is only available for Europe with a resolution of $0.0625° \times 0.0625°$ and is an outcome of the DLR-project 'Verkehrsentwicklung und Umwelt' (Hendricks et al., 2017).

The simulated period of the *REF* simulation ranges from 07/2007 to 12/2010. All sensitivity simulations are branched off

25 in 12/2007 from the *REF* simulation. The simulation period of the *EVEU* simulation ranges from 12/2007 to 12/2010. The simulation periods of the other simulations are given in Table 2. Due to the high computational resources needed for the CM12 model instance, the CM12 instance is only activated for the period May to August 2008 and only for the simulations *REF* and *EVEU* (see also Fig. S14).

All chemical species, as well as the tagging diagnostics, are initialised from a 6-month spin-up simulation with EMAC

30 only (period 01/2007–07/2007). This spin-up simulation was initialised with trace gas mixing ratios from the *RC1SD-base-10a* simulation described in detail by Jöckel et al. (2016). The soil-model TERRA of COSMO/MESSy is initialised with an output of a simulation without chemistry for the period 01/1983–07/2007. Further, MECO(n) is operated in the so called quasi chemistry transport model mode (QCTM-mode, Deckert et al., 2011; Mertens et al., 2016). In this mode chemistry and dynamics are decoupled to increase the signal-to-noise ratio for small chemical perturbations. For this climatologies are used

35 within EMAC: (a) for all radiatively active substances (CO_2, CH_4, N_2O, CFC-11 and CFC-12) for the radiation calculations,

(b) nitric acid (heterogeneous chemistry; submodel MSBM (Multiphase Stratospheric Box Model) and (c) for OH, O^1D and Cl for methane oxidation in the stratosphere (submodel CH4). In COSMO/MESSy only the climatology of nitric acid for the submodel MSBM is required. The applied climatologies are monthly mean values from the *RC1SD-base-10a* simulation.

For our comparison we focus on the period June–August (JJA) where the ozone production is largest. Further, we compare the results on the coarsest grid. Of course the finer resolved model instances provide additional information compared to the coarse model. On the grid of the finer model, however, the coarser model does not gain any information. Therefore, we investigate if the fine model provides an added value compared to the coarse model, on the grid of the coarse model.

3 Difference in Ozone Production

In a first step, we analyse the difference of the ozone production (for the *REF* simulation) simulated by EMAC and CM50, respectively. For this, we consider the net ozone production (P_{O3}) defined as:

$$P_{O3} = \mathrm{ProdO3} - \mathrm{LossO3}, \tag{1}$$

with the production ($\mathrm{ProdO3}$) and loss rates ($\mathrm{LossO3}$) as diagnosed by the chemical solver (for more details see Supplement of Grewe et al. (2017)).

We define ΔP_{O3} as $\Delta P_{O3} = P_{O3}^{\mathrm{CM50}} - P_{O3}^{\mathrm{EMAC}}$. ΔP_{O3} is largest in lower troposphere (see Fig. 2a). As indicated by the negative numbers, CM50 simulates in general lower values of P_{O3} than EMAC. Zonally averaged P_{O3} is around 60 to 80 $\mathrm{fmol\ mol^{-1}\ s^{-1}}$ lower in CM50 as in EMAC, which corresponds to 10–20 %. The largest differences (up to 100 $\mathrm{fmol\ mol^{-1}\ s^{-1}}$ or 40 %) are simulated over the Mediterranean See (see also Fig. S1 in the Supplement).

To separate effects caused by the emission inventory resolution from the effects caused by the model resolution and specific model biases, Fig. 2b shows the differences of ΔP_{O3} between the *ET42* and *REF* simulation ($\Delta P_{O3}^{\mathrm{ET42}} - \Delta P_{O3}^{\mathrm{REF}}$). The positive values indicate the effect of increased P_{O3} with reduced resolution of the emission inventory, which is caused by the dilution effect of the emissions on the coarse grid (e.g., Tie et al., 2010). The differences are largest in the Mediterranean area with an increase of P_{O3} in CM50 of up to 40 $\mathrm{fmol\ mol^{-1}\ s^{-1}}$ in *REF* compared to *ET42*. These differences are mainly simulated in the areas of the Alboran Sea and Balearic Sea, as well as in the areas of the Levantine Sea (see also Fig. S2 in the Supplement). The main reason for these differences are the dilution of the shipping emissions, and the large anthropogenic emissions in Israel if coarse emissions are applied. As the ozone production is strongly non-linear this dilution of the emissions leads to an artificial increase of the ozone production rate.

The other differences are caused by a variety of other model factors, which cannot be disentangled. Some of these factors are model specific temperature biases, differences of the land use classes, which affects loss processes (like dry deposition) or differences in vertical mixing (see Mertens et al., 2016).

Geoscientific
Model Development
Discussions

Table 1. Overview of the most important submodels applied in EMAC and COSMO/MESSy, respectively. Both COSMO/MESSy instances use the same set of submodels. MMD* comprises the MMD2WAY submodel and the MMD library.

Submodel	EMAC	COSMO	short description	references
AEROPT	x		calculation of aerosol optical properties	Dietmüller et al. (2016)
AIRSEA	x	x	exchange of tracers between air and sea	Pozzer et al. (2006)
CH4	x		methane oxidation and feedback to hydrological cycle	
CLOUD	x		cloud parametrisation	Roeckner et al. (2006), Jöckel et al. (2006)
CLOUDOPT	x		cloud optical properties	Dietmüller et al. (2016)
CONVECT	x		convection parametrisation	Tost et al. (2006b)
CVTRANS	x	x	convective tracer transport	Tost et al. (2010)
DDEP	x	x	dry deposition of aerosols and tracer	Kerkweg et al. (2006a)
E2COSMO	x		additional ECHAM5 fields for COSMO coupling	Kerkweg and Jöckel (2012b)
GWAVE	x		parametrisation of non-orographic gravity waves	Roeckner et al. (2003)
JVAL	x	x	calculation of photolysis rates	Landgraf and Crutzen (1998), Jöckel et al. (2006)
LNOX	x		NO_x-production by lighting	Tost et al. (2007), Jöckel et al. (2010)
MECCA	x	x	tropospheric and stratospheric gas-phase chemistry	Sander et al. (2011), Jöckel et al. (2010)
MMD*	x	x	coupling of EMAC and COSMO/MESSy (including libraries and all submodels)	Kerkweg and Jöckel (2012b); Kerkweg et al. (2018)
MSBM	x	x	multiphase chemistry of the stratosphere	Jöckel et al. (2010)
OFFEMIS	x	x	prescribed emissions of trace gases and aerosols	Kerkweg et al. (2006b)
ONEMIS	x	x	on-line calculated emissions of trace gases and aerosols	Kerkweg et al. (2006b)
ORBIT	x	x	Earth orbit calculations	Dietmüller et al. (2016)
QBO	x		Newtonian relaxation of the quasi-biennial oscillation (QBO)	Giorgetta and Bengtsson (1999), Jöckel et al. (2006)
RAD	x		radiative transfer calculations	Dietmüller et al. (2016)
SCAV	x	x	wet deposition and scavenging of trace gases and aerosols	Tost et al. (2006a)
SEDI	x	x	sedimentation of aerosols	Kerkweg et al. (2006a)
SORBIT	x	x	sampling along sun synchronous satellite orbits	Jöckel et al. (2010)
SURFACE	x		surface properties	Jöckel et al. (2016)
TAGGING	x	x	Source apportionment using a TAGGING method	Grewe et al. (2017)
TNUDGE	x	x	Newtonian relaxation of tracers	Kerkweg et al. (2006b)
TROPOP	x	x	diagnostic calculation of tropopause height and additional diagnostics	Jöckel et al. (2006)

Table 2. Overview of the applied simulation set-ups and simulation periods. For EMAC the same set-up is applied in all simulations, but the set-up of COSMO (both for CM50 and CM12) is varied systematically. More details are given in the text. The note 'calculated by EMAC' in the row 'biogenic emissions' means that the emissions, which are calculated by EMAC, are transformed to the COSMO grid during runtime via the MMD2WAY submodel.

Simulation		EMAC		COSMO	
acronym	period	anthropogenic emissions	biogenic emissions	anthropogenic emissions	biogenic emissions
REF	07/2007-12/2010			MACCity, $0.5°$ x $0.5°$	on-line calculated
ET42	12/2007-12/2008	MACCity, $2.8°$ x $2.8°$	on-line calculated	MACCity, $2.8°$ x $2.8°$	on-line calculated
EBIO	07/2007-12/2008			MACCity, $0.5°$ x $0.5°$	calculated by EMAC
EVEU	12/2007-12/2010			VEU, $0.0625°$ x $0.0625°$	on-line calculated
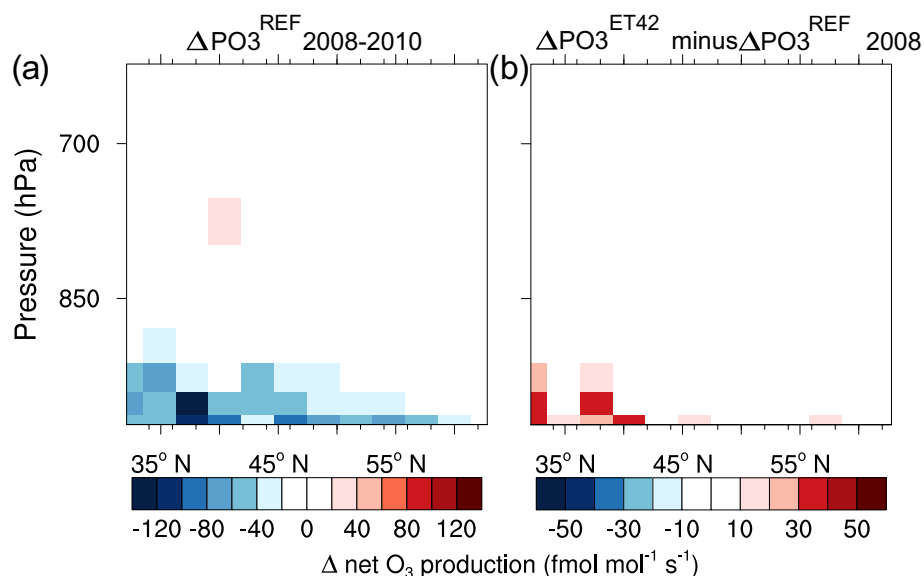
Figure 2. Zonally averaged differences of P_{O3} (ΔP_{O3}) between CM50 and EMAC (in $\mathrm{fmol\ mol^{-1}\ s^{-1}}$). **(a)** ΔP_{O3} calculated from the results of the *REF* simulation for JJA 2008–2010. **(b)** differences of ΔP_{O3} between the *ET42* and *REF* simulations for the year 2008 only. The CM50 data have been transformed on the horizontal and vertical grid of EMAC.

4 Contributors to ozone in Europe

Figure 3 shows the absolute and relative contributions of different emission sources to the European ozone column up to 850 hPa (see Table S1 in the Supplement for detailed definition of the tagging categories). The largest absolute and relative ozone contributors are the anthropogenic non-traffic and the biogenic categories, both with contributions of more than 1 DU corresponding to more than 15 %. Both models simulate similar absolute ozone contributions of the categories anthropogenic non-traffic ($\approx$ 1.0 DU), land transport ($\approx$ 0.7 DU), ship ($\approx$ 0.5 DU) and biomass burning ($\approx$ 0.4 DU). For the biogenic
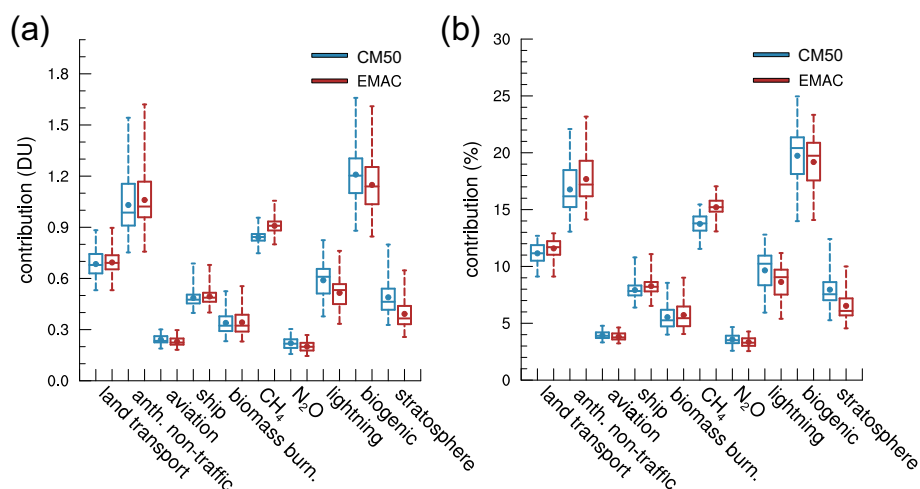
Figure 3. Box and whisker plot for the absolute (a, in DU) and relative (b, in %) contribution to the ozone column up to 850 hPa. The values are area-averaged over the CM50 domain. The lower and upper ends of the boxes indicates the 25th and 75th percentiles, the bars the medians, the dots the average and the whiskers the ranges of the timeseries for the JJA values from 2008–2010.

category, CM50 calculates slightly larger absolute contributions compared to EMAC (see Sect. 4.2), but the differences are small compared to the temporal variability of the contributions. Further, CM50 calculates larger absolute contributions of the categories lighting and stratosphere. Due to increased vertical mixing in CM50 compared to EMAC ozone which is produced in the upper troposphere is transported downward more efficiently. This leads to overall larger ozone columns up to 850 hPa

5   in CM50 compared to EMAC (Mertens et al., 2016). Therefore, EMAC simulates, despite similar absolute contributions of the anthropogenic categories, slightly larger relative contributions for these categories. Accordingly, CM50 simulates larger relative contributions to near ground-level ozone of the categories lightning and stratosphere compared to EMAC. These, however, are averages on continental scale. In a next step the differences of the geographical distribution are analysed in more detail. Here, we focus on the categories land transport, as one important anthropogenic emission source, and biogenic emissions (for all

10   other categories the differences are shown in Fig. S3 in the Supplement). As discussed in Sect. 2, the biogenic emissions are calculated on-line by both models depending on the meteorology and surface properties. While the total emissions are comparable, the geographical distribution, as well as the area averaged contribution, differ. As differences of on-line simulated emissions are a typical inter model difference, a detailed investigation of the influence of these differences is of interest.

4.1 Contribution of land transport emissions to ground level ozone

15   Averaged over JJA 2008 and the European area (defined as rectangular box from $10°$ W: $30°$ E and $32°$ N: $65°$ N, see red square in Fig. 1) EMAC simulates a relative contribution of the land transport emissions (denoted as O_3^{tra}) to ground level ozone of 13.1 %, while CM50 calculates a contribution of 11.9 %. A decrease of the emission resolution in CM50 increases the relative contribution to 12.1 % (*ET42* simulation), and the change of the anthropogenic emission inventory in CM50 increases
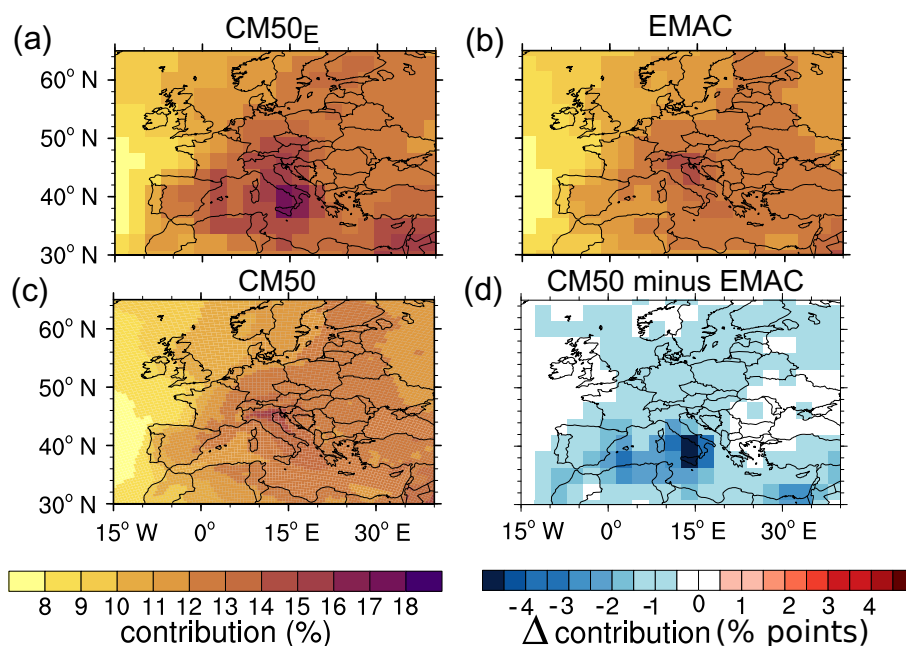
Figure 4. Comparison of the JJA averaged relative contribution of O_3^{tra} to groundlevel O_3 (in %) of EMAC and CM50: **(a)** results of EMAC, **(b)** results of CM50 transformed onto the EMAC grid, **(c)** results of CM50 on the original grid and **(d)** difference ('CM50 minus EMAC' in percentage points) on the coarse grid. **(a)**– **(c)** use the same (left) colour bar. Shown are the results of the *REF* simulation, averaged for 2008–2010.

the contribution to 12.7 % (*EVEU* simulation). In all cases similar absolute contributions of O_3^{tra} are simulated which range between 6.0 and 6.4 $\mathrm{nmol\ mol^{-1}}$. Accordingly, the area averaged values indicate that the inter-model differences between CM50 and EMAC have a larger influence on the calculated contributions than the change of the anthropogenic emission inventory. The impact of the coarsely resolved emission inventory on the area averaged values is rather small. In general, the

5   differences of the average contributions of O_3^{tra} simulated by the two models (EMAC and COSMO), as well as simulated by COSMO for the four different simulations are ≈ 10 % at maximum. In comparison to this, the inter-model differences of the contributions to ground-level O_3 with respect to the categories lightning and stratosphere, which result mainly from the differences of the dynamics, are much larger (≈ 20 % and ≈ 30 %, respectively).

   Regionally, the differences in relative contribution of O_3^{tra} to ground level ozone (see Fig. 4) can be larger than the area

10   averaged differences. In general, both models simulate a comparable distribution with the largest relative contribution of O_3^{tra} in the Mediterranean region and contributions of around 8 % over the western Atlantic. As discussed before, CM50 simulates over large parts of Europe a 0.5–1 percentage points lower relative contribution compared to EMAC, mainly caused by a decreased net ozone production and a stronger vertical mixing in CM50 compared to EMAC. With altitude the differences between EMAC and CM50 decrease (see Fig. S4 in the Supplement).

Geoscientific
Model Development
Discussions

The largest differences of the relative contribution of O_3^{tra} to ground level ozone are simulated around the Mediterranean area. The differences over the Mediterranean Sea (up to 2 percentage points and more, corresponding to more than 10 percent) can partly be attributed to the coarse resolution of the emissions in EMAC compared to CM50. As the analyses of the *ET42* simulation results shows, the coarse resolution leads to an artificial increase of P_{O3} which in turn leads to an increase of the

5   contribution from O_3^{tra} (and other anthropogenic categories). Accordingly, the results of CM50 of the *ET42* simulation shows regionally up to 3 nmol mol^{-1} and 3 percentage points larger contributions as the *REF* simulation (see also Fig. S5 in the Supplement). However, especially the large differences over Southern Italy and Sicily between CM50 and EMAC can not be attributed to the coarse resolution of the emissions. Here, EMAC simulates the largest contribution (up to 17 %) in the European region (especially around the Naples region with large land transport emissions), while CM50 simulates contributions of around

10   13 %. On the coarse EMAC grid most parts of Southern Italy are considered as sea, affecting especially the calculation of dry deposition in EMAC, as dry deposition of ozone is lower over sea as over land. Therefore, the coarse resolution of the land sea mask in EMAC compared to CM50 leads to an artificial underestimation of the loss. In addition, the coarse land sea mask leads to differences in the calculation of biogenic emissions. Especially over Sicily, EMAC simulates no biogenic emissions (including soil-NO_x) while CM50 simulates large emissions here (see Fig. S8 in the Supplement). Accordingly, soil-NO_x

15   and anthropogenic NO_x do not compete in EMAC in this area and ozone is mostly formed from anthropogenic emissions. Compared to this artificial peak produced by EMAC around Naples and over Sicily, CM50 shows the largest contribution (up to 15 %) around the Po basin. In this region, large amounts of emissions by land transport take place and ozone production is enhanced by stable and sunny weather conditions.

    The further increase of resolution from 50 km (CM50) to 12 km (CM12) impacts ozone and the contributions of ozone only

20   slightly (see Fig. S10 in the Supplement). In general, we note a decrease of the absolute ozone values, as well as the absolute contribution of anthropogenic emissions (including the land transport category) near the hotspot regions (e.g. Rhine-Ruhr, Munich, and Frankfurt), if the model resolution is increased (*REF* simulation). The increase of the resolution of the emission inventory (*EVEU* simulation) intensifies this effect, i.e. near the hotspots ozone values and absolute contributions of O_3^{tra} decrease further. In Southern and Eastern Germany, however, the ozone values increase. Especially in Southern Germany this

25   is mainly caused by the better resolved topography and larger contributions of stratospheric ozone. Accordingly, the absolute contribution of land transport emissions to ground level ozone decreases in this area.

    Focusing on the relative contribution of O_3^{tra} to groundlevel O_3 averaged over Germany we note a decrease in CM12 compared to CM50 (see Fig. 5). The difference is largest in Southern Germany, however, mostly below 0.5 percentage points (corresponding to less than 5 %). As discussed above, this is mainly caused by increased ozone of stratospheric origin. Fur-

30   ther, in Western Germany CM12 simulates a larger contribution of the CH_4 category to ozone compared to CM50, which is consistent with the larger tropospheric oxidation capacity in CM12 compared to CM50 (Mertens et al., 2016).

    In general, however, the differences of the contributions of O_3^{tra} to ground level ozone for the 95th percentile (see Fig. S11 in the Supplement) and the mean between the results of CM12 and CM50 are much smaller compared to the differences caused by the different anthropogenic emissions inventory (e.g. the differences of the results of the *REF* and *EVEU* simulation).
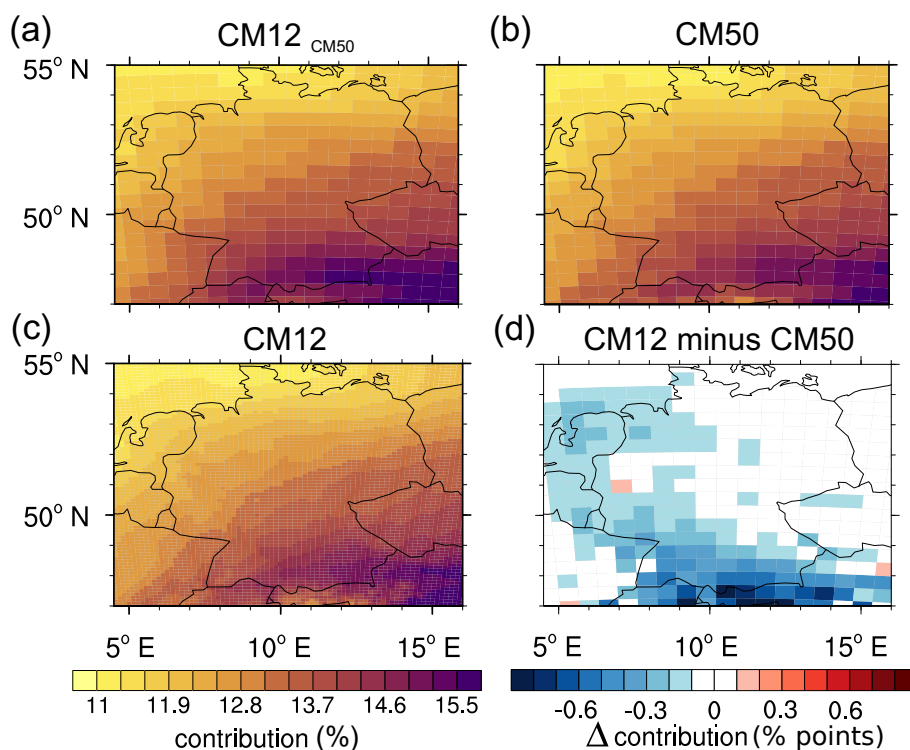
Figure 5. Comparison of the JJA averaged ground level contribution of O_3^{tra} to O_3 (in %) of CM50 and CM12: **(a)** results of CM50, **(b)** results of CM12 transformed onto the CM50 grid, **(c)** results of CM12 on the original grid and **(d)** difference ('CM12 minus CM50' in percentage points) on the coarse grid. **(a)–(c)** use the same (left) colour bar. Shown are the results of the *EVEU* simulation, averaged for 2008.

Accordingly, the differences of emission inventories dominate over differences caused by the resolution of emission inventories and models when comparing the results of CM50 and CM12.

What is not discussed here in detail is the influence of the difference of the shorter lived species, e.g. NO_2 or the tagged contributions to NO_y, which largely differ between the two resolutions. Here, maxima (e.g. in Stuttgart or around the Rhine-5 Ruhr area) are displaced in the coarser resolution (CM50) compared to the finer resolution (CM12). However, the direct influence of displaced precursors on ozone itself is not very large, because ozone formation usually takes place downwind of the source itself. Further, compared to previous studies investigating the influence of the model/emission inventory resolution on ozone (e.g. Wild, 2007; Tie et al., 2010; Markakis et al., 2015), it is important to note that we apply a chemistry-climate model in which not only the chemical processes are calculated on the finer grid, but also the meteorology. This can alter the 10 results compared to studies applying simpler chemistry-transport models.
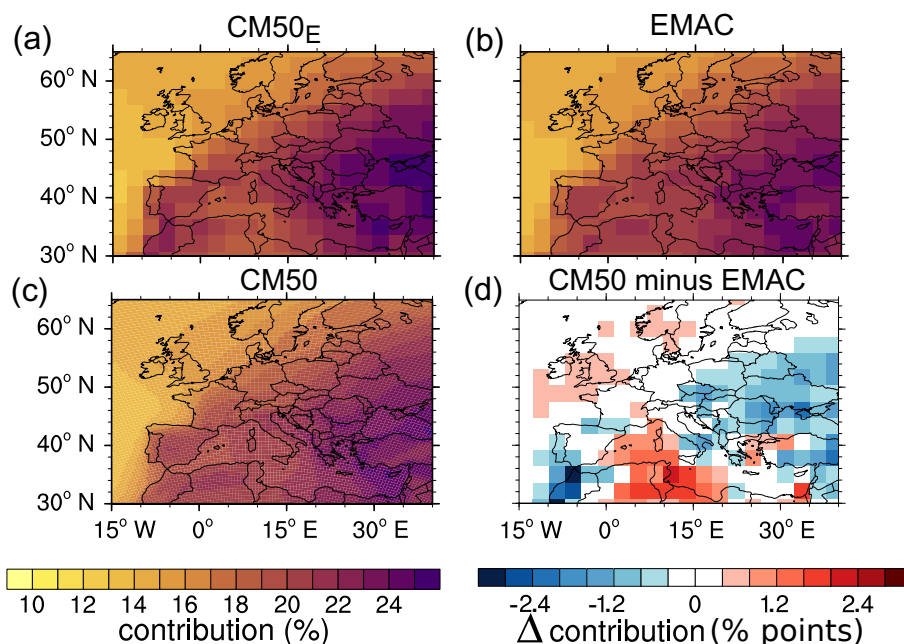
Figure 6. Comparison of the JJA averaged ground level contribution of O_3^{soi} to O_3 (in %) of EMAC and COSMO: **(a)** results of EMAC, **(b)** results of CM50 transformed onto the EMAC grid, **(c)** results of CM50 on the original grid and **(d)** difference ('CM50 minus EMAC' in percentage points) on the coarse grid. **(a)**– **(c)** use the same (left) colour bar. Shown are the results of the *REF* simulation, averaged for 2008–2010.

4.2 Contribution of biogenic emissions to ground level ozone

The JJA 2008 averaged relative contribution of ozone from biogenic emissions (mainly soil-NO_x and biogenic C_5H_8, denoted as O_3^{soi}) to ground level O_3 over the rectangular box defined as Europe (see Sect. 4.1) range from 19.0 to 19.6 % in all simulations. Hence, the differences of the relative contribution of O_3^{soi} to ground level ozone on the continental scale are rather small (below 5 %). The same is true for the absolute values, ranging from 9.3 to 9.7 nmol mol^{-1}.

With respect to the geographical distribution (Fig. 6) both models simulate a strong North-West to South-East gradient with relative contributions from O_3^{tra} of around 10 % over the Atlantic and more than 20 % over South-Eastern Europe. In contrast to the contribution of O_3^{tra}, EMAC does not show generally larger contributions of the biogenic category than CM50. Instead, EMAC simulates (in case of the *REF* simulation larger contributions (1–2 percentage points) over South-Eastern Europe and Morocco/Iberian Peninsula, while CM50 simulates around 1–2 percentage points larger contributions over large parts of the Mediterranean Sea as well as over Northern Africa. Also around the British Islands and Norway, the relative contributions of O_3^{soi} simulated by CM50 are larger by around 0.5 percentage points compared to EMAC. In total, CM50 ends up with 0.5 percentage points larger contributions of O_3^{soi} compared to EMAC. Similar as for the land transport category,

the differences between the results of both models decrease with increasing height, but the general pattern stay similarly (see Figs. S7 in the Supplement).

The differences between EMAC and CM50 are only partly caused by the different geographical distribution of the biogenic emissions in EMAC compared to CM50. When applying the same biogenic emissions as in EMAC in CM50 (*EBIO* simulation

5 the relative and absolute contributions of O_3^{soi} are increased mainly in the Mediterranean area by up to 2 percentage points and 3 nmol mol^{-1}, respectively. The characteristic dipole pattern between EMAC and CM50, however, stays similar but the maximum is reduced (see Fig. S8 and Fig. S9 in the Supplement). These differences are mainly caused by inter-model differences.

In general, we conclude that regionally differences of the relative and absolute contribution of O_3^{soi} caused by inter-model

10 differences, emission resolution as well as different geographical distribution are up to 15 %. Averaged over Europe the differences are lower (10 %). Again, the differences are lower as for example the differences of around 30 % observed for the differences of the contributions to ozone from the stratosphere.

5 Discussion

So far, the results indicate that with respect to average values on continental scale, the differences caused by the resolution of

15 the model/emission inventory are rather small. This confirms findings by Stock et al. (2013), reporting only a small influence of the global redistribution of megacity emissions (which can be seen as a locally decreased emission resolution) on the global ozone budget.

To summarise and quantify these differences in more detail, Fig. 7 shows the absolute (a) and relative (b) contributions of O_3^{tra} to ground level ozone for the whole CM50 domain, as well as for the regions defined in the Prudence project (Christensen

20 et al., 2007). Figure 7 shows that also on the scale of smaller regions, the absolute and the relative contribution of O_3^{tra} to ground-level ozone is only slightly influenced by the coarse resolution of anthropogenic emission inventories (*ET42*) as well as by a different geographical location or resolution of biogenic emissions (*EBIO*). This does not only hold for the mean O_3^{tra} contributions, but also for the extreme values expressed by the 95th percentile. Also the simulated differences for the biogenic and shipping category, which are affected much more by the changed variations of the emission inventories in the two

25 simulations, are rather small (see Fig. S12 and Fig. S13 in the Supplement). The largest simulated differences of the contribution of shipping emissions to ground-level ozone between the *REF*, *EBIO* and *ET42* simulation are around 0.5 nmol mol^{-1} and below 0.5 percentage points, respectively. The largest change (95th percentile) of the biogenic category in the region Iberian Peninsula is around 0.7 nmol mol and 0.5 percentage − points, respectively.

Compared to the differences of the contribution of O_3^{tra} between the *REF*, *ET42*, and *EBIO*, the differences caused by a

30 changed emission inventory (*EVEU*) are larger. In the Mediterranean region, the mean and 95th percentile of the contribution of O_3^{tra} increases by 1 nmol mol^{-1} and 2 percentage points, respectively. In the Alps region the increase of the 95th percentile of the contribution is up to 1.3 nmol mol^{-1} and 3 percentage points, respectively. Similarly, also for the contribution of shipping emissions the differences are largest with the changed emission inventory (up to 1.5 nmol mol^{-1} and 1 percentage
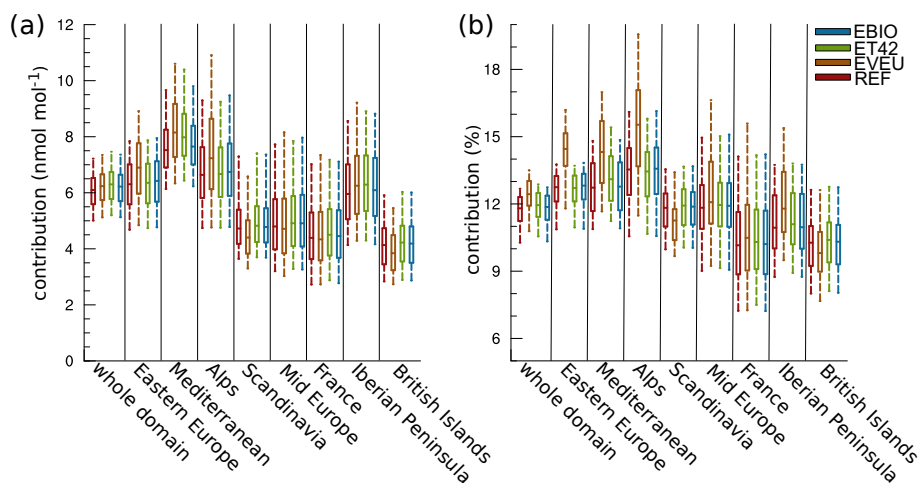
Geoscientific
Model Development
Discussions

Open Access

Figure 7. Comparison of the contributions of O_3^{tra} to ground level ozone for JJA 2008 between the four simulations. (a) displays the absolute contribution in $nmol\ mol^{-1}$ and (b) the relative contribution to ground level ozone (in %). All values are area averaged over the respective region and are calculated using the results of the CM50 instance. The lower and upper end of the box indicate the 25th and 75th percentile, respectively, the bar the median, and the whiskers the 5th and 95th percentile of the timeseries for the JJA values from 2008 based on 3-hourly model output.

point). Accordingly, changes in the resolution of the emission inventory or the biogenic emissions can effect the contribution of anthropogenic categories (such as land transport and shipping). However, on the regional scale the main drivers of uncertainties are clearly the anthropogenic emissions as well as inter model differences. As an example we found regional differences (cf. Sect. 4.1) of the contribution of O_3^{tra} to ground level O_3 between EMAC and CM50 of up to 20 % around the Naples region.

6 Summary and Conclusions

In the present study, we are focusing on the question "Are contributions of emissions to ozone a matter of scale?'. To answer this question we compare the influence of the model, the model resolution, the emission resolution and the emission inventory on the results of ozone contribution analyses. For this we apply the MECO(n) model system which combines a global and a regional model by means of an on-line nesting technique. By applying the identical tagging diagnostics (source apportionment method) in the regional and global model and consistent boundary conditions, we are able to compare the results of model instances with different resolutions to investigate the influence of the model and emission inventory resolutions onto the diagnosed ozone contributions. Such analyses are important to quantify uncertainties of ozone source apportionment studies, which arise due to limitations of the model and/or computational resources.

Our comparison showed, that with respect to ozone contributions on continental scale (e.g. Europe) the differences simulated by our global and our regional model and two specific anthropogenic emission inventories are rather small. The largest differences of the contribution of anthropogenic emission sources was up to 10 % for the contribution of land transport emissions to

ground level ozone. However, the contribution of stratospheric ozone to ground level ozone calculated by EMAC and COSMO differs by up to 30 %, suggesting that inter-model differences with respect to downward transport of ozone can be larger.

Consistent with previous studies, a coarser resolution of the emission inventory and/or of the model increases on average the ozone mixing ratios and the absolute contributions of emission sources to ozone. However, the relative contributions to ozone
5 change only slightly. In general, the difference caused by the emission inventory resolution are smaller than differences arising from the different models and emission inventories.

Accordingly, the answer to the questions in the title is a clear 'it depends'. Questions such as 'What is the average contribution of land transport emissions to ozone over Europe' can be answered with a global model and/or coarser resolved emissions, taking into account positively biased absolute contributions. On the regional scale, however, inter-model differences (caused
10 partly by the model resolution) as well as effects introduced by specific emission inventories or the emission inventory resolution can be much larger. For the investigated combinations of models and emissions we observed differences of up to 20 % for the contributions of land transport emissions to ground level ozone. Further, maxima are shifted by misplaced emissions or coarsely resolved land sea masks due to the coarser resolution of the emission inventories or the models. These effects arise mainly near hotspot regions like the Po basin or near major shipping routes in the Mediterranean Sea. However, especially in
15 these areas contribution analyses of anthropogenic emissions are very important and effects like artificially increased ozone levels and contributions caused by coarse resolution of models and or emission inventories should be avoided.

Further, this study shows how the application of a source apportionment method helps in explaining differences between the results of different models or model configurations. In this case, the larger ground level ozone mixing ratios simulated by COSMO compared to EMAC can partly be explained by a more efficient vertical mixing, which is supported by a larger
20 contribution of the stratospheric ozone at ground level simulated by COSMO compared to EMAC.

Clearly, this study is only a first step to quantify the driving sources of uncertainties and especially the role of the model and emission inventory resolutions on the results of ozone contribution studies. Especially, as some processes like vertical diffusion or transport can heavily alter the model results, follow up studies need to take into account more (and more different) models to better estimate the inter-model differences when applying source apportionment methods. In addition, the two analysed
25 anthropogenic emission inventories clearly do not reflect the whole spectrum of different emission estimates. Further, our analyses focused only on differences near the origin of the emissions. An increased resolution leads to a more realistic chemistry within the plumes downwind of the emission hotspots. This can affect the long range transport from different precursors and might influence regions far away from the emission region. Especially calculations of radiative forcings are very sensitive to ozone near the tropopause. In a coarsely resolved model, the overestimated absolute contributions might lead to a biased
30 radiative forcing. This effect, however, is difficult to quantify and would require very fine resolved global chemistry climate models or 2-way-nesting capabilities, which feed back information about the contributions from the fine back to the coarse grid. For a next step a further increase of the model and emission resolution should be envisaged. Even if we found only small differences between 50 and 12 km resolution this step would be important, as even with a 12 km grid resolution emissions are diluted over large areas. A finer resolution could reduce the dilution strongly. Such an analysis, however, is hindered by two
35 aspects: First, consistent emission inventories (anthropogenic and natural) with a resolution of 1 km over areas, which are large

enough to compare models on regional and global scale must be available. Second, requirements with respect to computational time of chemistry-climate models with ≈ 1 km resolution over large computational domains are very demanding, hindering detailed quantification of the differences caused by the resolution over long integration periods.

Geoscientific
Model Development
Discussions

References

Butler, T., Lupascu, A., Coates, J., and Zhu, S.: TOAST 1.0: Tropospheric Ozone Attribution of Sources with Tagging for CESM 1.2.2, Geoscientific Model Development, 11, 2825–2840, https://doi.org/10.5194/gmd-11-2825-2018, https://www.geosci-model-dev.net/11/2825/2018/, 2018.

5 Christensen, J. H., Carter, T. R., Rummukainen, M., and Amanatidis, G.: Evaluating the performance and utility of regional climate models: the PRUDENCE project, Climatic Change, 81, 1–6, https://doi.org/10.1007/s10584-006-9211-6, http://dx.doi.org/10.1007/s10584-006-9211-6, 2007.

Clappier, A., Belis, C. A., Pernigotti, D., and Thunis, P.: Source apportionment and sensitivity analysis: two methodologies with two different purposes, Geoscientific Model Development, 10, 4245–4256, https://doi.org/10.5194/gmd-10-4245-2017, https://www.geosci-model-dev.net/10/4245/2017/, 2017.

Dahlmann, K., Grewe, V., Ponater, M., and Matthes, S.: Quantifying the contributions of individual NOx sources to the trend in ozone radiative forcing, Atmos. Environ., 45, 2860–2868, https://doi.org/http://dx.doi.org/10.1016/j.atmosenv.2011.02.071, http://www.sciencedirect.com/science/article/pii/S1352231011002366, 2011.

Deckert, R., Jöckel, P., Grewe, V., Gottschaldt, K.-D., and Hoor, P.: A quasi chemistry-transport model mode for EMAC, Geosci. Model Dev., 4, 195–206, https://doi.org/10.5194/gmd-4-195-2011, http://www.geosci-model-dev.net/4/195/2011/, 2011.

Dee, D. P., Uppala, S. M., Simmons, A. J., Berrisford, P., Poli, P., Kobayashi, S., Andrae, U., Balmaseda, M. A., Balsamo, G., Bauer, P., Bechtold, P., Beljaars, A. C. M., van de Berg, L., Bidlot, J., Bormann, N., Delsol, C., Dragani, R., Fuentes, M., Geer, A. J., Haimberger, L., Healy, S. B., Hersbach, H., Hólm, E. V., Isaksen, L., Kållberg, P., Köhler, M., Matricardi, M., McNally, A. P., Monge-Sanz, B. M., Morcrette, J.-J., Park, B.-K., Peubey, C., de Rosnay, P., Tavolato, C., Thépaut, J.-N., and Vitart, F.: The ERA-Interim reanalysis: configuration and performance of the data assimilation system, Quart. J. Roy. Meteor. Soc., 137, 553–597, https://doi.org/10.1002/qj.828, http://dx.doi.org/10.1002/qj.828, 2011.

Dietmüller, S., Jöckel, P., Tost, H., Kunze, M., Gellhorn, C., Brinkop, S., Frömming, C., Ponater, M., Steil, B., Lauer, A., and Hendricks, J.: A new radiation infrastructure for the Modular Earth Submodel System (MESSy, based on version 2.51), Geoscientific Model Development, 9, 2209–2222, https://doi.org/10.5194/gmd-9-2209-2016, http://www.geosci-model-dev.net/9/2209/2016/, 2016.

25 Dunker, A. M., Yarwood, G., Ortmann, J. P., and Wilson, G. M.: Comparison of Source Apportionment and Source Sensitivity of Ozone in a Three-Dimensional Air Quality Model, Environmental Science & Technology, 36, 2953–2964, https://doi.org/10.1021/es011418f, http://dx.doi.org/10.1021/es011418f, pMID: 12144273, 2002.

Emmons, L. K., Hess, P. G., Lamarque, J.-F., and Pfister, G. G.: Tagged ozone mechanism for MOZART-4, CAM-chem and other chemical transport models, Geosci. Model Dev., 5, 1531–1542, https://doi.org/10.5194/gmd-5-1531-2012, http://www.geosci-model-dev.net/5/1531/2012/, 2012.

Eyring, V., Stevenson, D. S., Lauer, A., Dentener, F. J., Butler, T., Collins, W. J., Ellingsen, K., Gauss, M., Hauglustaine, D. A., Isaksen, I. S. A., Lawrence, M. G., Richter, A., Rodriguez, J. M., Sanderson, M., Strahan, S. E., Sudo, K., Szopa, S., van Noije, T. P. C., and Wild, O.: Multi-model simulations of the impact of international shipping on Atmospheric Chemistry and Climate in 2000 and 2030, Atmos. Chem. Phys., 7, 757–780, https://doi.org/10.5194/acp-7-757-2007, http://www.atmos-chem-phys.net/7/757/2007/, 2007.

35 Fiore, A. M., J., D. F., O., W., Cuvelier, C., Schultz, M. G., Hess, P., Textor, C., Schulz, M., Doherty, R., Horowitz, L., MacKenzie, I., Sanderson, M., Shindell, D., S., S. D., S., S., R., V. D., G., Z., C., A., D., B., I., B., G., C., J., C. W., N., D. B., G., F., G., F., M., G., S., G., D., H., T., H., A., I. I. S., J., J. D., E., J. J., W., K. J., J., K. T., A., L., E., M., V., M., J., P. R., G., P., J., P. K., A., P. J., S., S., G.,

Geoscientific
Model Development
Discussions

V. M., P., W., G., W., S., W., and A., Z.: Multimodel estimates of intercontinental source-receptor relationships for ozone pollution, Journal of Geophysical Research: Atmospheres, 114, https://doi.org/10.1029/2008JD010816, https://agupubs.onlinelibrary.wiley.com/doi/abs/10.1029/2008JD010816, 2009.

Fiore, A. M., Naik, V., Spracklen, D. V., Steiner, A., Unger, N., Prather, M., Bergmann, D., Cameron-Smith, P. J., Cionni, I., Collins,
5   W. J., Dalsøren, S., Eyring, V., Folberth, G. A., Ginoux, P., Horowitz, L. W., Josse, B., Lamarque, J.-F., MacKenzie, I. A., Nagashima, T., O'Connor, F. M., Righi, M., Rumbold, S. T., Shindell, D. T., Skeie, R. B., Sudo, K., Szopa, S., Takemura, T., and Zeng, G.: Global air quality and climate, Chem. Soc. Rev., 41, 6663–6683, https://doi.org/10.1039/C2CS35095E, http://dx.doi.org/10.1039/C2CS35095E, 2012.

Giorgetta, M. A. and Bengtsson, L.: Potential role of the quasi-biennial oscillation in the stratosphere-troposphere exchange as found in
10   water vapor in general circulation model experiments, J. Geophys. Res. Atmos., 104, 6003–6019, https://doi.org/10.1029/1998JD200112, http://dx.doi.org/10.1029/1998JD200112, 1999.

Granier, C., Bessagnet, B., Bond, T., D'Angiola, A., van der Gon, H. D., Frost, G., Heil, A., Kaiser, J., Kinne, S., Klimont, Z., Kloster, S., Lamarque, J.-F., Liousse, C., Masui, T., Meleux, F., Mieville, A., Ohara, T., Raut, J.-C., Riahi, K., Schultz, M., Smith, S., Thompson, A., Aardenne, J., Werf, G., and Vuuren, D.: Evolution of anthropogenic and biomass burning emissions of air pollutants at global and regional
15   scales during the 1980–2010 period, Clim. Change, 109, 163–190, 2011.

Grewe, V.: The origin of ozone, Atmos. Chem. Phys., 6, 1495–1511, https://doi.org/10.5194/acp-6-1495-2006, http://www.atmos-chem-phys.net/6/1495/2006/, 2006.

Grewe, V., Tsati, E., Mertens, M., Frömming, C., and Jöckel, P.: Contribution of emissions to concentrations: the TAGGING 1.0 submodel based on the Modular Earth Submodel System (MESSy 2.52), Geoscientific Model Development, 10, 2615–2633,
20   https://doi.org/10.5194/gmd-10-2615-2017, https://www.geosci-model-dev.net/10/2615/2017/, 2017.

Guenther, A., Hewitt, C., E., D., Fall, R. G., C., Graedel, T., Harley, P., Klinger, L., Lerdau, M., McKay, W., Pierce, T., S., B., Steinbrecher, R., Tallamraju, R., Taylor, J., and Zimmermann, P.: A global model of natural volatile organic compound emissions, J. Geophys. Res., 100, 8873–8892, 1995.

Hendricks, J., Righi, M., Dahlmann, K., Gottschaldt, K.-D., Grewe, V., Ponater, M., Sausen, R., Heinrichs, D., Winkler, C., Wolfermann, A.,
25   Kampffmeyer, T., Friedrich, R., Klötzke, M., and Kugler, U.: Quantifying the climate impact of emissions from land-based transport in Germany, Transportation Research Part D: Transport and Environment, https://doi.org/https://doi.org/10.1016/j.trd.2017.06.003, 2017.

Hofmann, C., Kerkweg, A., Wernli, H., and Jöckel, P.: The 1-way on-line coupled atmospheric chemistry model system MECO(n) Part 3: Meteorological evaluation of the on-line coupled system, Geosci. Model Dev., 5, 129–147, https://doi.org/10.5194/gmd-5-129-2012, http://www.geosci-model-dev.net/5/129/2012/, 2012.

30   Holmes, C. D., Prather, M. J., and Vinken, G. C. M.: The climate impact of ship NO_x emissions: an improved estimate accounting for plume chemistry, Atmospheric Chemistry and Physics, 14, 6801–6812, https://doi.org/10.5194/acp-14-6801-2014, http://www.atmos-chem-phys.net/14/6801/2014/, 2014.

Hoor, P., Borken-Kleefeld, J., Caro, D., Dessens, O., Endresen, O., Gauss, M., Grewe, V., Hauglustaine, D., Isaksen, I. S. A., Jöckel, P., Lelieveld, J., Myhre, G., Meijer, E., Olivie, D., Prather, M., Schnadt Poberaj, C., Shine, K. P., Staehelin, J., Tang, Q., van Aardenne, J., van
35   Velthoven, P., and Sausen, R.: The impact of traffic emissions on atmospheric ozone and OH: results from QUANTIFY, Atmos. Chem. Phys., 9, 3113–3136, https://doi.org/10.5194/acp-9-3113-2009, http://www.atmos-chem-phys.net/9/3113/2009/, 2009.

Huang, M., Carmichael, G. R., Pierce, R. B., Jo, D. S., Park, R. J., Flemming, J., Emmons, L. K., Bowman, K. W., Henze, D. K., Davila, Y., Sudo, K., Jonson, J. E., Tronstad Lund, M., Janssens-Maenhout, G., Dentener, F. J., Keating, T. J., Oetjen, H., and Payne, V. H.: Impact of

intercontinental pollution transport on North American ozone air pollution: an HTAP phase 2 multi-model study, Atmospheric Chemistry and Physics, 17, 5721–5750, https://doi.org/10.5194/acp-17-5721-2017, https://www.atmos-chem-phys.net/17/5721/2017/, 2017.

Jöckel, P., Sander, R., Kerkweg, A., Tost, H., and Lelieveld, J.: Technical Note: The Modular Earth Submodel System (MESSy) - a new approach towards Earth System Modeling, Atmos. Chem. Phys., 5, 433–444, https://doi.org/10.5194/acp-5-433-2005, http://www.
5   atmos-chem-phys.net/5/433/2005/, 2005.

Jöckel, P., Tost, H., Pozzer, A., Brühl, C., Buchholz, J., Ganzeveld, L., Hoor, P., Kerkweg, A., Lawrence, M., Sander, R., Steil, B., Stiller, G., Tanarhte, M., Taraborrelli, D., van Aardenne, J., and Lelieveld, J.: The atmospheric chemistry general circulation model ECHAM5/MESSy1: consistent simulation of ozone from the surface to the mesosphere, Atmos. Chem. Phys., 6, 5067–5104, https://doi.org/10.5194/acp-6-5067-2006, http://www.atmos-chem-phys.net/6/5067/2006/, 2006.

10 Jöckel, P., Kerkweg, A., Pozzer, A., Sander, R., Tost, H., Riede, H., Baumgaertner, A., Gromov, S., and Kern, B.: Development cycle 2 of the Modular Earth Submodel System (MESSy2), Geosci. Model Dev., 3, 717–752, https://doi.org/10.5194/gmd-3-717-2010, http://www.geosci-model-dev.net/3/717/2010/, 2010.

Jöckel, P., Tost, H., Pozzer, A., Kunze, M., Kirner, O., Brenninkmeijer, C. A. M., Brinkop, S., Cai, D. S., Dyroff, C., Eckstein, J., Frank, F., Garny, H., Gottschaldt, K.-D., Graf, P., Grewe, V., Kerkweg, A., Kern, B., Matthes, S., Mertens, M., Meul, S., Neumaier, M., Nützel, M.,
15 Oberländer-Hayn, S., Ruhnke, R., Runde, T., Sander, R., Scharffe, D., and Zahn, A.: Earth System Chemistry integrated Modelling (ES-CiMo) with the Modular Earth Submodel System (MESSy) version 2.51, Geosci. Model Dev., 9, 1153–1200, https://doi.org/10.5194/gmd-9-1153-2016, http://www.geosci-model-dev.net/9/1153/2016/, 2016.

Karamchandani, P., Long, Y., Pirovano, G., Balzarini, A., and Yarwood, G.: Source-sector contributions to European ozone and fine PM in 2010 using AQMEII modeling data, Atmospheric Chemistry and Physics, 17, 5643–5664, https://doi.org/10.5194/acp-17-5643-2017,
20 https://www.atmos-chem-phys.net/17/5643/2017/, 2017.

Kerkweg, A. and Jöckel, P.: The 1-way on-line coupled atmospheric chemistry model system MECO(n) Part 1: Description of the limited-area atmospheric chemistry model COSMO/MESSy, Geosci. Model Dev., 5, 87–110, https://doi.org/10.5194/gmd-5-87-2012, http://www.geosci-model-dev.net/5/87/2012/, 2012a.

Kerkweg, A. and Jöckel, P.: The 1-way on-line coupled atmospheric chemistry model system MECO(n) - Part 2: On-line coupling with the
25 Multi-Model-Driver (MMD), Geosci. Model Dev., 5, 111–128, https://doi.org/10.5194/gmd-5-111-2012, http://www.geosci-model-dev.net/5/111/2012/, 2012b.

Kerkweg, A., Buchholz, J., Ganzeveld, L., Pozzer, A., Tost, H., and Jöckel, P.: Technical Note: An implementation of the dry removal processes DRY DEPosition and SEDImentation in the Modular Earth Submodel System (MESSy), Atmos. Chem. Phys., 6, 4617–4632, https://doi.org/10.5194/acp-6-4617-2006, http://www.atmos-chem-phys.net/6/4617/2006/, 2006a.

30 Kerkweg, A., Sander, R., Tost, H., and Jöckel, P.: Technical note: Implementation of prescribed (OFFLEM), calculated (ONLEM), and pseudo-emissions (TNUDGE) of chemical species in the Modular Earth Submodel System (MESSy), Atmos. Chem. Phys., 6, 3603–3609, https://doi.org/10.5194/acp-6-3603-2006, http://www.atmos-chem-phys.net/6/3603/2006/, 2006b.

Kerkweg, A., Hofmann, C., Jöckel, P., Mertens, M., and Pante, G.: The on-line coupled atmospheric chemistry model system MECO(n) – Part 5: Expanding the Multi-Model-Driver (MMD v2.0) for 2-way data exchange including data interpolation via GRID (v1.0), Geoscien-
35 tific Model Development, 11, 1059–1076, https://doi.org/10.5194/gmd-11-1059-2018, https://www.geosci-model-dev.net/11/1059/2018/, 2018.

Kwok, R. H. F., Baker, K. R., Napelenok, S. L., and Tonnesen, G. S.: Photochemical grid model implementation and application of VOC, NO_x, and O_3 source apportionment, Geoscientific Model Development, 8, 99–114, https://doi.org/10.5194/gmd-8-99-2015, http://www.geosci-model-dev.net/8/99/2015/, 2015.

Landgraf, J. and Crutzen, P. J.: An efficient method for online calculations of photolysis and heating rates., J. Atmos. Sci., 55, 863–878, https://doi.org/http://dx.doi.org/10.1175/1520-0469, 1998.

Lelieveld, J. and Dentener, F. J.: What controls tropospheric ozone?, J. Geophys. Res. Atmos., 105, 3531–3551, https://doi.org/10.1029/1999JD901011, http://dx.doi.org/10.1029/1999JD901011, 2000.

Li, Y., Lau, A. K.-H., Fung, J. C.-H., Zheng, J. Y., Zhong, L. J., and Louie, P. K. K.: Ozone source apportionment (OSAT) to differentiate local regional and super-regional source contributions in the Pearl River Delta region, China, Journal of Geophysical Research: Atmospheres, 117, https://doi.org/10.1029/2011JD017340, http://dx.doi.org/10.1029/2011JD017340, d15305, 2012.

Markakis, K., Valari, M., Perrussel, O., Sanchez, O., and Honore, C.: Climate-forced air-quality modeling at the urban scale: sensitivity to model resolution, emissions and meteorology, Atmospheric Chemistry and Physics, 15, 7703–7723, https://doi.org/10.5194/acp-15-7703-2015, https://www.atmos-chem-phys.net/15/7703/2015/, 2015.

Matthes, S., Grewe, V., Sausen, R., and Roelofs, G.-J.: Global impact of road traffic emissions on tropospheric ozone, Atmos. Chem. Phys., 7, 1707–1718, https://doi.org/10.5194/acp-7-1707-2007, http://www.atmos-chem-phys.net/7/1707/2007/, 2007.

Matthias, V., Aulinger, A., Backes, A., Bieser, J., Geyer, B., Quante, M., and Zeretzke, M.: The impact of shipping emissions on air pollution in the greater North Sea region – Part 2: Scenarios for 2030, Atmos. Chem. Phys., 16, 759–776, https://doi.org/10.5194/acp-16-759-2016, http://www.atmos-chem-phys.net/16/759/2016/, 2016.

Mertens, M., Kerkweg, A., Jöckel, P., Tost, H., and Hofmann, C.: The 1-way on-line coupled model system MECO(n) – Part 4: Chemical evaluation (based on MESSy v2.52), Geoscientific Model Development, 9, 3545–3567, https://doi.org/10.5194/gmd-9-3545-2016, http://www.geosci-model-dev.net/9/3545/2016/, 2016.

Mertens, M., Grewe, V., Rieger, V. S., and Jöckel, P.: Revisiting the contribution of land transport and shipping emissions to tropospheric ozone, Atmospheric Chemistry and Physics, 18, 5567–5588, https://doi.org/10.5194/acp-18-5567-2018, https://www.atmos-chem-phys.net/18/5567/2018/, 2018.

Mertens, M. B.: Contribution of road traffic emissions to tropospheric ozone in Europe and Germany, http://nbn-resolving.de/urn:nbn:de:bvb:19-207288, 2017.

Pöschl, U., von Kuhlmann, R., Poisson, N., and Crutzen, P.: Development and Intercomparison of Condensed Isoprene Oxidation Mechanisms for Global Atmospheric Modeling, J. Atmos. Chem., 37, 29–152, https://doi.org/10.1023/A:1006391009798, http://dx.doi.org/10.1023/A%3A1006391009798, 2000.

Pozzer, A., Jöckel, P., Sander, R., Williams, J., Ganzeveld, L., and Lelieveld, J.: Technical Note: The MESSy-submodel AIRSEA calculating the air-sea exchange of chemical species, Atmos. Chem. Phys., 6, 5435–5444, https://doi.org/10.5194/acp-6-5435-2006, http://www.atmos-chem-phys.net/6/5435/2006/, 2006.

Price, C. and Rind, D.: A simple lightning parameterization for calculating global lightning distributions, J. Geophys. Res. Atmos., 97, 9919–9933, https://doi.org/10.1029/92JD00719, http://dx.doi.org/10.1029/92JD00719, 1992.

Rockel, B., Will, A., and Hense, A.: The Regional Climate Model COSMO-CLM (CCLM), Meteorol. Z., 17, 347–348, 2008.

Roeckner, E., Bäuml, G., Bonaventura, L., Brokopf, R., Esch, M., Giorgetta, M., Hagemann, S., Kirchner, I., Kornblueh, L., Manzini, E., Rhodin, A., Schlese, U., Schulzweida, U., and Tompkins, A.: The atmospheric general circulation model ECHAM5.

PART I: Model description, MPI-Report 349, Max Planck Institut für Meteorologie in Hamburg, Deutschland, available at: https://www.mpimet.mpg.de/fileadmin/publikationen/Reports/max_scirep_349.pdf (last access: 18 October 2015), 2003.

Roeckner, E., Brokopf, R., Esch, M., Giorgetta, M., Hagemann, S., Kornblueh, L., Manzini, E., Schlese, U., and Schulzweida, U.: Sensitivity of Simulated Climate to Horizontal and Vertical Resolution in the ECHAM5 Atmosphere Model, J. Climate, 19, 3771–3791, https://doi.org/10.1175/jcli3824.1, http://dx.doi.org/10.1175/jcli3824.1, 2006.

Sander, R., Baumgaertner, A., Gromov, S., Harder, H., Jöckel, P., Kerkweg, A., Kubistin, D., Regelin, E., Riede, H., Sandu, A., Taraborrelli, D., Tost, H., and Xie, Z.-Q.: The atmospheric chemistry box model CAABA/MECCA-3.0, Geosci. Model Dev., 4, 373–380, https://doi.org/10.5194/gmd-4-373-2011, http://www.geosci-model-dev.net/4/373/2011/, 2011.

Stock, Z. S., Russo, M. R., Butler, T. M., Archibald, A. T., Lawrence, M. G., Telford, P. J., Abraham, N. L., and Pyle, J. A.: Modelling the impact of megacities on local, regional and global tropospheric ozone and the deposition of nitrogen species, Atmos. Chem. Phys., 13, 12 215–12 231, https://doi.org/10.5194/acp-13-12215-2013, http://www.atmos-chem-phys.net/13/12215/2013/, 2013.

Tie, X., Brasseur, G., and Ying, Z.: Impact of model resolution on chemical ozone formation in Mexico City: application of the WRF-Chem model, Atmos. Chem. Phys., 10, 8983–8995, https://doi.org/10.5194/acp-10-8983-2010, http://www.atmos-chem-phys.net/10/8983/2010/, 2010.

Tost, H., Jöckel, P., Kerkweg, A., Sander, R., and Lelieveld, J.: Technical note: A new comprehensive SCAVenging submodel for global atmospheric chemistry modelling, Atmos. Chem. Phys., 6, 565–574, https://doi.org/10.5194/acp-6-565-2006, http://www.atmos-chem-phys.net/6/565/2006/, 2006a.

Tost, H., Jöckel, P., and Lelieveld, J.: Influence of different convection parameterisations in a GCM, Atmos. Chem. Phys., 6, 5475–5493, https://doi.org/10.5194/acp-6-5475-2006, http://www.atmos-chem-phys.net/6/5475/2006/, 2006b.

Tost, H., Jöckel, P., and Lelieveld, J.: Lightning and convection parameterisations – uncertainties in global modelling, Atmos. Chem. Phys., 7, 4553–4568, https://doi.org/10.5194/acp-7-4553-2007, http://www.atmos-chem-phys.net/7/4553/2007/, 2007.

Tost, H., Lawrence, M. G., Brühl, C., Jöckel, P., The GABRIEL Team, and The SCOUT-O3-DARWIN/ACTIVE Team: Uncertainties in atmospheric chemistry modelling due to convection parameterisations and subsequent scavenging, Atmos. Chem. Phys., 10, 1931–1951, https://doi.org/10.5194/acp-10-1931-2010, http://www.atmos-chem-phys.net/10/1931/2010/, 2010.

Valverde, V., Pay, M. T., and Baldasano, J. M.: Ozone attributed to Madrid and Barcelona on-road transport emissions: Characterization of plume dynamics over the Iberian Peninsula, Science of The Total Environment, 543, Part A, 670 – 682, https://doi.org/http://dx.doi.org/10.1016/j.scitotenv.2015.11.070, http://www.sciencedirect.com/science/article/pii/S0048969715310500, 2016.

Wang, Y., Jacob, D. J., and Logan, J. A.: Global simulation of tropospheric O3-NOx-hydrocarbon chemistry: 3. Origin of tropospheric ozone and effects of nonmethane hydrocarbons, Journal of Geophysical Research: Atmospheres, 103, 10 757–10 767, https://doi.org/10.1029/98JD00156, https://agupubs.onlinelibrary.wiley.com/doi/abs/10.1029/98JD00156, 1998.

Wild, O.: Modelling the global tropospheric ozone budget: exploring the variability in current models, Atmospheric Chemistry and Physics, 7, 2643–2660, https://doi.org/10.5194/acp-7-2643-2007, http://www.atmos-chem-phys.net/7/2643/2007/, 2007.

Wild, O. and Prather, M. J.: Global tropospheric ozone modeling: Quantifying errors due to grid resolution, J. Geophys. Res. Atmos., 111, n/a–n/a, https://doi.org/10.1029/2005JD006605, http://dx.doi.org/10.1029/2005JD006605, d11305, 2006.

Yienger, J. J. and Levy, H.: Empirical model of global soil-biogenic NOx emissions, Journal of Geophysical Research: Atmospheres, 100, 11 447–11 464, https://doi.org/10.1029/95JD00370, http://dx.doi.org/10.1029/95JD00370, 1995.

Young, P. J., Archibald, A. T., Bowman, K. W., Lamarque, J.-F., Naik, V., Stevenson, D. S., Tilmes, S., Voulgarakis, A., Wild, O., Bergmann,
D., Cameron-Smith, P., Cionni, I., Collins, W. J., Dalsøren, S. B., Doherty, R. M., Eyring, V., Faluvegi, G., Horowitz, L. W., Josse, B.,
Lee, Y. H., MacKenzie, I. A., Nagashima, T., Plummer, D. A., Righi, M., Rumbold, S. T., Skeie, R. B., Shindell, D. T., Strode, S. A.,
Sudo, K., Szopa, S., and Zeng, G.: Pre-industrial to end 21st century projections of tropospheric ozone from the Atmospheric Chemistry
5   and Climate Model Intercomparison Project (ACCMIP), Atmos. Chem. Phys., 13, 2063–2090, https://doi.org/10.5194/acp-13-2063-2013,
http://www.atmos-chem-phys.net/13/2063/2013/, 2013.